

Observation of the interactions of silver nanoparticles (AgNPs) mediated by acid in the aquatic matrices using in-situ liquid cell transmission electron microscopy

Fernando, Ishara; Tay, Yee Yan; Karunasekera, Hasith; Zhou, Yan

2020

Fernando, I., Tay, Y. Y., Karunasekera, H. & Zhou, Y. (2020). Observation of the interactions of silver nanoparticles (AgNPs) mediated by acid in the aquatic matrices using in-situ liquid cell transmission electron microscopy. *Analytica Chimica Acta*, 1104, 47-52.

<https://dx.doi.org/10.1016/j.aca.2019.12.072>

<https://hdl.handle.net/10356/152049>

<https://doi.org/10.1016/j.aca.2019.12.072>

© 2019 Elsevier B.V. All rights reserved. This paper was published in *Analytica Chimica Acta* and is made available with permission of Elsevier B.V.

Downloaded on 05 Apr 2024 01:02:08 SGT

**Observation of the interactions of Silver nanoparticles (AgNPs) mediated
by acid in the aquatic matrices using in-situ liquid cell transmission
electron microscopy**

Ishara Fernando^{1,2}, Yee Yan Tay^{3,4}, Hasith Karunasekera⁵, Yan Zhou^{2,6*}

¹Interdisciplinary Graduate School, Nanyang Technological University, Singapore 639798.

²Nanyang Environment & Water Research Institute, Advanced Environmental Biotechnology
Centre, Nanyang Technological University, 1 Cleantech Loop, CleanTech One, Singapore
637141.

³Facility for Analysis, Characterization, Testing and Simulation, Nanyang Technological
University, 50 Nanyang Avenue, Singapore 639798.

⁴School of Materials Science and Engineering, College of Engineering, Nanyang
Technological University, 50 Nanyang Avenue, Singapore 639798

⁵School of Electrical & Electronic Engineering, College of Engineering, Nanyang
Technological University, Singapore 639798.

⁶School of Civil & Environmental Engineering, College of Engineering, Nanyang
Technological University, Singapore 639798.

*Corresponding author at: Tel.: +65 6790 6103; E-mail address: zhouyan@ntu.edu.sg

23 **Abstract**

24

25 The properties of the solution matrix play a prominent role in determining the interactions
26 between the silver nanoparticles (AgNPs) when they are present in the aquatic environment.
27 Here, using in situ liquid cell transmission electron microscopy (LCTEM), we show that the
28 interaction of AgNPs is predominantly affected by the solution pH. Reducing the pH in the
29 solution will accelerate the aggregation of AgNPs due to the alteration of the charge cloud
30 around the NPs. Aggregates formed in this scenario were non spherical and irregular shaped
31 and were stable under the electron beam irradiation. Individual AgNPs and smaller
32 aggregates moved randomly and approached the larger aggregates before the aggregation
33 process came to an end. We found that during the aggregation process, the mode of jump to
34 contact and the pairwise approach of aggregation differed according to the composition of the
35 solution. Observations made using the LCTEM were further explained using empirical
36 formulae. Our observation on the pH induced interactions provides important insights on
37 predicting the behavior of AgNPs released through many anthropogenic activities in the
38 environment.

39

40 **Keywords:** Liquid cell transmission electron microscopy, aggregation, interactions, Silver
41 nanoparticles

42

43 **Introduction**

44 Interactions between nanoparticles (NPs) in solution play an important role in understanding
45 their transformation and subsequent fate in engineered systems. For example, they are
46 responsible for colloidal stability [1], aggregation [2], dissolution [3] and reactions with
47 biological macromolecules [4]. These interactions are regulated by the attractive and
48 repulsive electrostatic forces between two interactive surfaces in water [5]. It is known that
49 these short-range forces may prevent the surfaces from approaching closer than several water
50 molecules [6]. However, the exact origin and mechanism of these forces is still not fully-
51 understood. For example, the classical continuum models account only for a repulsive diffuse
52 double layer and the attractive van der Waals (vdW) forces in the matrix [7]. Even though the
53 two macroscopic hydrophilic surfaces are just a short-distance apart, these forces may
54 dominate other intermolecular forces [8, 9]. It is unclear how the repulsive diffuse double
55 layer exactly affects the interaction dynamics of NPs.

56

57 The properties of the solution matrix, where silver NPs (AgNPs) are present, have a
58 significant impact on various interactions, such as absorption, oxidation reactions and
59 dissolution. Hence, determining the transformations of AgNPs, widely used in the consumer
60 products which are subsequently released into the aquatic environment [10] is critical.

61

62 Recently, the correlation between the pH with the colloidal stability, dissolution and
63 aggregation kinetic of these AgNPs has been evaluated [11]. This was done in the
64 environmentally relevant conditions from acidic to basic using different analytical techniques
65 such as UV vis, DLS and TEM. Empirical formulae have also been used to relate the
66 chemistry behind the phenomenon of aggregation of AgNPs with the experimental results. It

67 was found that AgNPs aggregated rapidly in the acidic conditions whereas they only
68 dissolved in the alkaline conditions.

69 The synthesized NPs will have their own surface charge when present in the
70 environment. The surface charges act like a cloud of electrons surrounding the NPs when the
71 latter is present in the liquid. It creates a metastable state, preventing the NPs from
72 aggregating to each other due to vdW forces. Therefore, when differentiating the interactions
73 of AgNPs in the absence and presence of acid, we found that the presence of acid in the
74 solution alter the surface charge of the AgNPs changing the electrostatic potential of the
75 AgNPs. Thus, this charge cloud is altered or disturbed affecting the stability of the NPs. As a
76 result, aggregation will take place. While the aggregation kinetics is recorded systematically
77 with time [11], there is little information on the path observation of the aggregation
78 interaction of the AgNPs in solution when the pH is varied. Path observation has been made
79 possible in the recent years using the in-situ liquid cell transmission electron microscopy
80 (LCTEM) [12], which can potentially be applied in geochemical and environmental studies.
81 LCTEM directly helps in quantifying and structuring the NPs dispersed in a solution, while
82 also simplifying the tracking of real-time interactions between individual NPs. Advantages of
83 using LCTEM include, firstly, the ability to visualize dynamic processes depending on the
84 total number of NPs. Secondly, it allows exploring how liquid flows through the cell and the
85 solution-properties that affect the interactions of NPs. Finally, with the capability to observe
86 such in-situ processes in the electron microscope, the presence of the electrostatic forces
87 between NPs, vital in the attachment [13], growth [14] and assembly [15] of NPs, is also
88 observable. In these studies, tracking the movement of interacting NPs within few
89 nanometers, showed that electrostatic interactions facilitate the pairwise approach and the
90 subsequent alignment of NPs. LCTEM enables investigating the impact of an external stimuli
91 directly on the interactions and the dynamics of NPs in a solution [16, 17].

The objectives of this study include (1) evaluating the mechanism of aggregation of AgNPs in water and acid with respect to the change in the interactive forces; (2) assessing the impact of intermolecular forces on interactions of NPs, and (3) appraising the suitability of LCTEM as a technique for in-situ studies in environment-related subjects. Here, using the in-situ LCTEM imaging [18-21], we visualized the time-resolved pH-induced dynamic interactions of AgNPs in water, showing that their mutual approach was hindered by the primary hydration shell of individual AgNPs.

Materials and Methods

The AgNPs used during the experiments were synthesized via oxidation-reduction of AgNO₃ using NaBH₄ [11] as mentioned in SI, characterized according to Fernando et al [22] and the typical size of the NPs used were about 40-75 nm.

Our experimental setup included a thin layer of liquid specimen [23] with AgNPs sandwiched between the two-electron transparent Silicon Nitride (Si₃N₄) membranes (~50nm thick on each side) of a liquid cell with the help of the Au spacer of (~50 nm) in thickness. The diffusion of NPs due to translation and rotation within these thin liquid films near liquid-solid interfaces is strongly suppressed [24, 25]. As such, the real time imaging and quantification of the interaction force fields of an otherwise rapid phenomenon can be facilitated.

We carried out the flow experiment using the Protochip Poseidon Liquid Cell Holder with two kinds of solutions: freshly-synthesized, uncoated 10 mg/L AgNP solution (final pH ~8) and 10% (w/v %) Nitric (V) acid solution. Before loading the AgNPs onto the grids, they were adequately rinsed using acetone and methanol at least for 5 min respectively. The e-

chips were, then, plasma-cleaned (3:1Argon/Oxygen mixture) for about 5 min using the Fishione Plasma Cleaner Nanoclean Model 1070 for surface treatment to change the Si_3N_4 membranes from hydrophobic to hydrophilic and to remove possible organic contaminants on the surfaces [26]. Right after the hydrophilic treatment, the sample of 0.3 μL was drop-cast onto the chips before sealing up for the experiment.

First, the AgNPs in the fluid cell e-chips were observed through the JEOL 2010 TEM with a high-resolution pole piece operated at 200 kV and the JEOL GrandARM TEM operated at 300 kV with a wide gap pole piece, mounted with an image corrector. The camera used are the AMT XR40B CCD (JEOL 2010HR) and Gatan Oneview CMOS camera (JEOL GrandARM) at a rate of 4-10 frames per second. The electron doses range from 0.75 to 58.5 $\text{e}/(\text{\AA}^2\cdot\text{s})$. In order to observe the aggregation dynamically, fresh AgNPs was first pumped through the liquid cell holder to the fluid cell using a syringe pump (Harvard Apparatus, Pump 11 Elite) at an infuse rate of 300 $\mu\text{l}/\text{h}$. After allowing ample time for the AgNPs to reach the fluid cell, the movement of AgNPs in the matrix was observed. Subsequently, Nitric (V) acid was pumped into the fluid cell using a syringe pump at an infuse rate of 150 $\mu\text{l}/\text{h}$. As such the observation of the aggregation occurs in a situation where the pH is continuously changing. The impact of the beam on the movement of NPs in liquid cells due to heating or momentum transfer from energetic electrons is negligible under these imaging conditions. However, charging during the imaging may enhance the movement of the NPs [27]. The images obtained during different scenario were processed as mentioned in SI.

Results and Discussion

Temporal observation on the mobility of the AgNPs in different environment

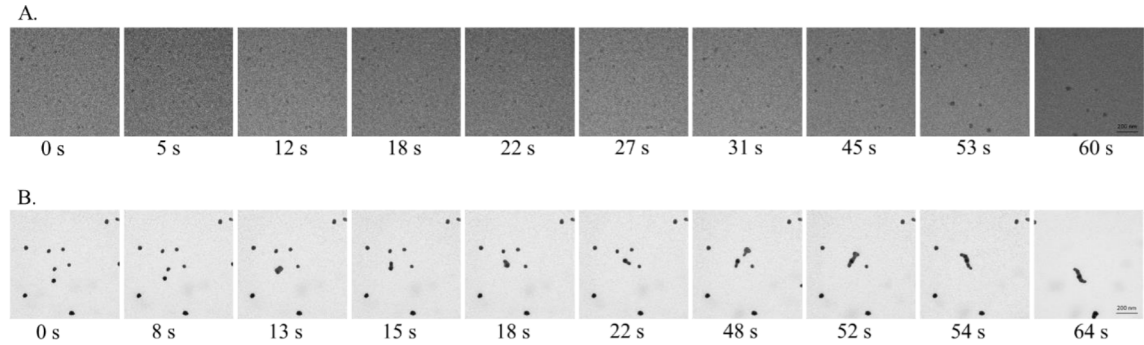
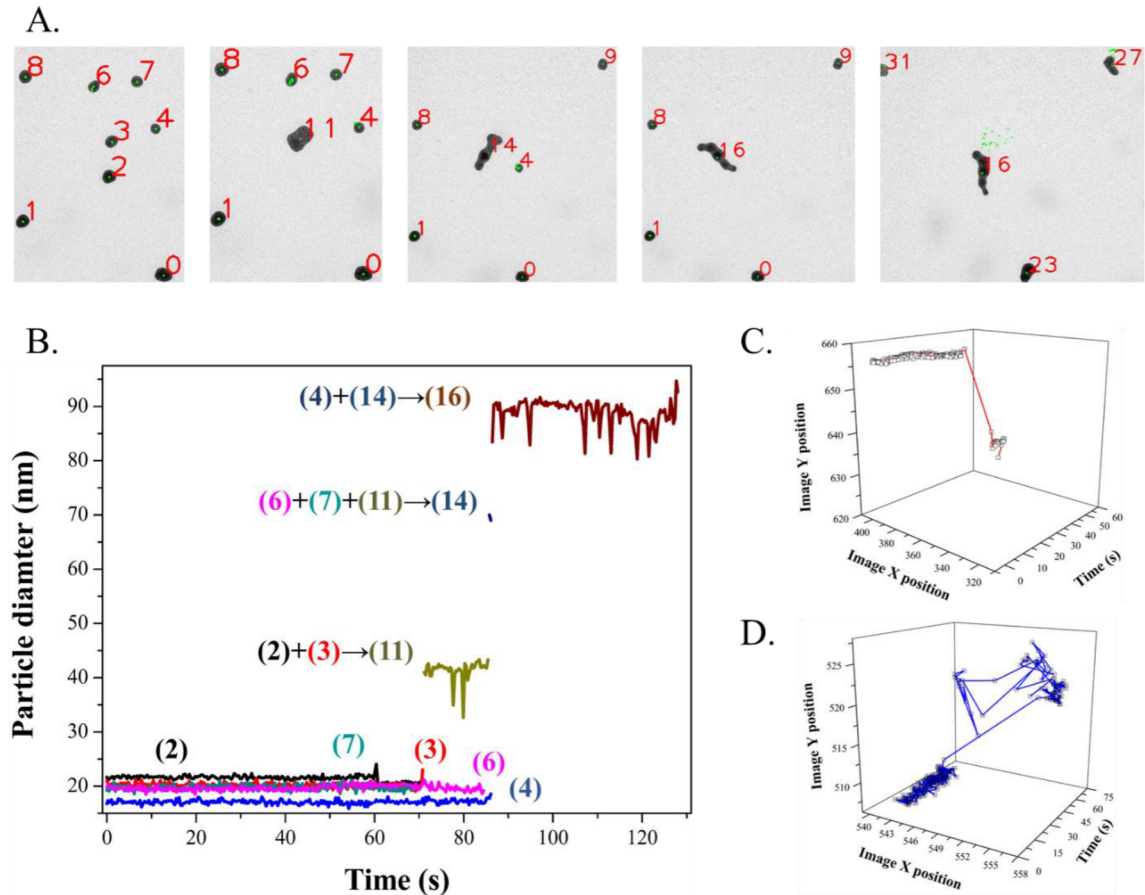


Figure 1. Time series images showing the interactions of individual AgNPs in the (A) deionized (DI) water and (B) in the presence of acid (processed images). AgNP concentration : 10 mg/L.

Time resolved TEM images of the AgNPs interacting in water (Figure 1A) are compared with those in the presence of acid (Figure 1B). According to Figure 1A, the distance between the single NPs and the clusters changed irregularly with time. It is also apparent from Movie S1 which demonstrates that the movement of AgNPs was non-directional, suggesting the random movement of AgNPs in the liquid over time. A striking difference between Figure 1A and 1B is the time-taken for the aggregation of AgNPs in water and in the presence of acid. It took longer for particle-aggregation in water (aggregation starts at 53s in water vs aggregation start at 13s in acid) compared to acid. The liquid cell holder was not electronically designed to measure the varying pH physically over the time while the acid/water was introduced during the experiment. pH was estimated based on an approximation using the flowrates, length of the tubes and the area of the chip. According to the approximation, the pH of the solution at the time where the images in the acidic condition of the Fig. 1B was taken lies around 5.5. This is also consistent with the result that was previously published using UV-vis

[11] where the spectra starts to indicate a change in the surface plasmon peak profile in the UV-vis spectrum with the reducing pH.

The distance between the single AgNPs decreased with time in the presence of the acid (Figure 1B). In addition, rotational and translational as well as translational-rotational coupled movements of these small AgNP aggregates were also observed (Movie 1 & 2). The change in the UV vis spectrum of the AgNPs with the solution pH is illustrated in Figure S4, which is also consistent with the LCTEM results. Variation in the solution pH also changed the behavior of the AgNPs resulting in rapid attachment of the smaller aggregates with each other forming larger aggregates consequently. Figure S3 shows the growth of these large aggregates of AgNPs changing with time in the presence of acid.



172

173 **Figure 2.** (A) Images with the tracking IDs showing movement of AgNPs in forming
174 aggregates, (B) the change in the particle diameter of the AgNPs in (A) in the acidic solution,
175 (C) Mobility of the particle with the Track ID (2) in (A) and (D) Mobility of the particle with
176 the Track ID (4) in (A). AgNP concentration: 10 mg/L.

177

178 We further evaluated the aggregation process for the AgNPs in the presence of acid (Figure
179 1B) by carefully tracking the individual particles. The TEM images of the AgNPs with
180 tracking IDs before and after the addition of Nitric (V) acid are shown in Figure 2A. At the
181 beginning, the NPs were distributed evenly within the field of view. Aggregation
182 subsequently happened with particles of different mobility albeit these AgNPs moved in
183 random directions before the attachment (Figure 2C & D). According to the Figure 2C & D,
184 the mobility exhibited by the particle with the track ID (4) was higher than that of the particle
185 with the track ID (2). Particle with the track ID (2), moved for a limited time as an individual
186 particle before aggregation. The particle with the tracking ID (4), however, moved randomly
187 for a considerable time before the aggregation as observed in Figure 2D.

188

189 **Interaction of AgNPs with Water vs Acid**

190

191 The random movements of the AgNPs and their attractive and repulsive interactions in water
192 are observed in Movie S1 such as some particles disappearing and reappearing again.
193 Furthermore, it is observed that the movement of the individual NPs in DI water is more
194 vigorous as compared to the one the acidic condition under similar dose of irradiation (SI
195 Movie 1 vs Movie 2). It is not clear why this happened but may be related to the explanation

as follows. Since the point of zero charge of bare Si₃N₄ is about pH 4.1, AgNPs initially adhered to the positively-charged Si₃N₄ membrane [28] when they were in the DI water ($pH \approx 6.5$), via electrostatic attraction and vdW forces. After several seconds of exposure to the electron beam, some of the particles or aggregates detached from the Si₃N₄ membrane and moved in a quasi 2D plane closer to the membrane in the focal plane making it visible under the TEM. This could be due to the increasingly negative electrical charges built up on the Si₃N₄ membrane and the secondary emission of the electron beam irradiation, the negatively charged AgNPs repulsed and detached from the membrane permanently, initiating the aggregation. Many of these observations can be described by the attractive forces between a membrane and the particles as expressed in Eqn. (1).

$$F = -\frac{k_A R}{6z^2} \quad (1)$$

Where k_A is the Hamaker constant of water which is 1.5×10^{-19} , R is the radius of the AgNPs or the aggregates and z is the distance between the membrane and the aggregate.

The charging of the Si₃N₄ membrane and NPs, which caused electrostatic repulsions between the membrane and the charged AgNP aggregates can be the driving force to the fast movement of the NPs and aggregates in the water (Figure 1A, Movie S1). On the other hand, due to the introduction of the acid, the presence of H⁺ can increase the conductivity of the solution and reduce the negative electrical charge built-up by the membrane. As the H⁺ ions have positive charges, the negative charges or the electrons attract towards them in the solution. Subsequently the charge cloud around the AgNPs will be destabilized resulting in a reduced and inhomogeneous amount of negative charges among the AgNPs, thus altering the resultant surface charge of the AgNPs. For further clarification, we have explained the phenomena in a pictorial way below in Figure 3.

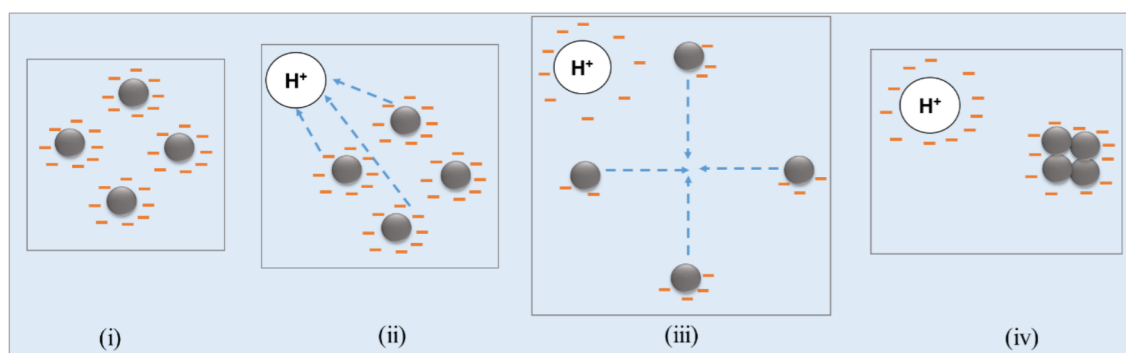


Figure 3. Mechanism involved in the change of the particle behavior with pH in acidic region

(i) AgNPs in the aquatic solution (ii) Introduction of a proton to the system (iii) Deterioration of the electron cloud around the particles and attraction of the electrons towards the proton (iv) Formation of the aggregates by the destabilized AgNPs which is enhanced by the increasing amount of protons

Moreover, aggregates with an increased size were observed in the presence of high concentration of H^+ ions, as the vdW attractive force between the AgNPs and Si_3N_4 membrane increased (Eqn.(1)). The addition of H^+ ions weakened this electrostatic repulsive force and decreased the distance (z) between the AgNPs. The interactive force between the membrane and the particles/aggregates is inversely proportional to z^2 (Eqn.(1)). Therefore, the increased traction from the membrane probably limited the random motion of the aggregates in the acidic solution. This phenomenon could suppress the detachment and mobility of the AgNPs.

As the aggregates grew considerably in size, such as the one observed in Figure S3, the larger aggregates were attracted strongly towards the membrane. Therefore, larger aggregates (Figure S3) were stationary during observation with the electrostatic repulsive force between the Si_3N_4 membrane and AgNPs being lower than the vdW attractive forces between the

membrane and the particles. There were, however, some remaining AgNPs and smaller aggregates moving continuously in a random manner (Figure S3).

Behavior of aggregation of AgNPs

As we temporally resolved the difference in the way AgNPs behave in different environments and their mobility difference, it is also possible to observe the difference in the movement of the NP aggregates in the solution using LCTEM and considering these other interactions are worthwhile. For example, we observed the randomly-moving AgNPs jumped back and forth several times before aggregation between AgNPs occurred in water (Figure 1A). Such behavior of AgNPs in water can be explained in the following way. Each of the AgNP aggregate was enclosed in a repulsive and anisotropic charge cloud in water. When the repulsive clouds of two AgNPs or aggregates overlapped, they approached each other closely. According to Movie S1 & Figure 1A, individual NPs moved nearer to the aggregates and approached them from different directions before the aggregation. As the AgNPs were nearer to each other, the individual AgNPs were repulsed by the repulsive cloud of the aggregates. AgNPs would then try different ways to overcome the energy barrier for interaction such as the rotation and translational behavior of these individual AgNPs. It is not clear why in the end the AgNPs aggregated despite that the solution pH was around 8. It might be due to the radiolysis of the solution by the electron beam which produced different radicals reducing the pH locally[29]. When the repulsive forces between the charged NPs were finally screened, the stronger short-range attractive vdW forces enable the particles to aggregate.

In the presence of acid, the aggregation behavior and mechanism are different from the one in DI water. As shown in Figure 1B (Figure 1B, Movie S2), in the acidic environment,

individual AgNPs exhibited directional interaction with each other and had interesting aggregation behavior. We observed that in the presence of the H^+ ions, as the distance between the isolated AgNPs changed, the pairwise interactions can be observed initially. Then, it promoted the AgNPs to form multiple pairwise aggregates. The pairwise distance (coupling proximity) changed differently depicting the change in the solution matrix affecting the interactions. Thereafter, these multiple pairwise aggregates rotated first before aggregating with each other or other AgNPs indicating the presence of a directional interaction behavior. Followed by the formation of multiple paired AgNPs, a sudden jump occurred, allowing these paired AgNPs to contact each other, which resulted in the mutual attachment of these AgNP-pairs increasing their overall diameter (Figure 2B). The observation shows that aggregation of individual AgNPs increased in the presence of H^+ ions at the same concentration of AgNPs (Figure 1A vs 1B), although the mobility reduces with increasing aggregate-sizes (Figure 1B vs S3). This establishes that the presence of H^+ ions affected the aggregation state of the individual AgNPs and aggregates, determining their interactions in the solution.

It is likely that the origin of the aggregation mechanism is due to the electrostatic repulsion being screened in the presence of H^+ ions (Figure 1B). The short-range interactions between the aggregates were dominated by the vdW attractions, which facilitated the final attachment process. On the other hand, the long-range attractions would take place when the distance between two AgNPs become larger than the range of the vdW forces. These long-range attractions are usually observed between identically charged NPs in confined geometries [30] similar to the liquid cell used in the LCTEM study. The long-range attractions are mediated by the redistribution of the ions and counter ions by the confining walls in the solution around the AgNPs, becoming the driving force for two AgNPs or aggregates to move together.

Therefore, the long-range, like-charge attractions and the short-range vdW attractions worked together in governing the direct attachment of AgNPs and smaller aggregates to the larger aggregates in the presence of H^+ ions. This finding could give insights in understanding how the change in the size of the aggregates affect their colloidal stability and toxicity [31] in the environmental matrices.

Conclusions

This study reveals that randomly moving AgNPs in an aquatic matrix tend to aggregate due to the repulsive electrostatic and attractive vdW forces. The aggregation of AgNPs induced by the chemical composition of the solution matrix will have important implications on the kinetics of the transformations of the AgNPs in the aquatic environment. The difference in the time taken for the inter-particle attachment in these two scenarios indicates that the jump-to-contact phenomenon observed during particle-attachment occurs almost instantaneously when the electron layer around the AgNPs is affected, which is governed by the properties of the solution such as acidity. The formation of transient pairs before the direct contact may provide enough time for AgNPs to change their orientation and explore optimal configuration to attach completely. This phenomenon may be critical in different processes such as the oriented-attachment of crystals or site-specific binding between biological macromolecules. We believe that future studies exploiting LCTEM will provide important insights into details of interaction mechanisms among other properties of the solution matrix and the AgNPs, which will be important in the areas of environmental science and engineering.

Conflicts of interest

There are no conflicts to declare.

Acknowledgement

The authors are grateful for the assistance received during the experiments from the Facility for Analysis, Characterization, Testing and Simulation at Nanyang Technological University, Singapore.

References

- [1] R.I. MacCusprie, Colloidal stability of silver nanoparticles in biologically relevant conditions, *Journal of Nanoparticle Research*, 13 (2011) 2893-2908.
- [2] A.M.E. Badawy, T.P. Luxton, R.G. Silva, K.G. Scheckel, M.T. Suidan, T.M. Tolaymat, Impact of Environmental Conditions (pH, Ionic Strength, and Electrolyte Type) on the Surface Charge and Aggregation of Silver Nanoparticles Suspensions, *Environmental Science & Technology*, 44 (2010) 1260-1266.
- [3] X. Li, J.J. Lenhart, Aggregation and Dissolution of Silver Nanoparticles in Natural Surface Water, *Environmental Science & Technology*, 46 (2012) 5378-5386.
- [4] C. Levard, E.M. Hotze, G.V. Lowry, G.E. Brown Jr, Environmental transformations of silver nanoparticles: impact on stability and toxicity, *Environmental Science & Technology*, 46 (2012) 6900-6914.
- [5] J. Israelachvili, H. Wennerström, Role of hydration and water structure in biological and colloidal interactions, *Nature*, 379 (1996) 219.
- [6] U. Anand, J. Lu, D. Loh, Z. Aabdin, U. Mirsaidov, Hydration Layer-Mediated Pairwise Interaction of Nanoparticles, *Nano Letters*, 16 (2016) 786-790.
- [7] V. Parsegian, T. Zemb, Hydration forces: Observations, explanations, expectations, questions, *Current opinion in colloid & interface science*, 16 (2011) 618-624.

339 [8] J.P. Cleveland, T. Schäffer, P.K. Hansma, Probing oscillatory hydration potentials using
 340 thermal-mechanical noise in an atomic-force microscope, *Physical Review B*, 52 (1995)
 341 R8692.

342 [9] J.I. Kilpatrick, S.-H. Loh, S.P. Jarvis, Directly probing the effects of ions on hydration
 343 forces at interfaces, *Journal of the American Chemical Society*, 135 (2013) 2628-2634.

344 [10] E.M. Hotze, T. Phenrat, G.V. Lowry, Nanoparticle Aggregation: Challenges to
 345 Understanding Transport and Reactivity in the Environment, *Journal of Environmental*
 346 *Quality*, 39 (2010) 1909-1924.

347 [11] I. Fernando, Y. Zhou, Impact of pH on the stability, dissolution and aggregation kinetics
 348 of silver nanoparticles, *Chemosphere*, 216 (2019) 297-305.

349 [12] J. Park, H. Zheng, W.C. Lee, P.L. Geissler, E. Rabani, A.P. Alivisatos, Direct
 350 observation of nanoparticle superlattice formation by using liquid cell transmission electron
 351 microscopy, *Acs Nano*, 6 (2012) 2078-2085.

352 [13] Q. Chen, H. Cho, K. Manthiram, M. Yoshida, X. Ye, A.P. Alivisatos, Interaction
 353 Potentials of Anisotropic Nanocrystals from the Trajectory Sampling of Particle Motion
 354 using in Situ Liquid Phase Transmission Electron Microscopy, *ACS Central Science*, 1
 355 (2015) 33-39.

356 [14] J.E. Evans, K.L. Jungjohann, N.D. Browning, I. Arslan, Controlled growth of
 357 nanoparticles from solution with in situ liquid transmission electron microscopy, *Nano*
 358 *letters*, 11 (2011) 2809-2813.

359 [15] Y. Liu, X.-M. Lin, Y. Sun, T. Rajh, In situ visualization of self-assembly of charged
 360 gold nanoparticles, *Journal of the American Chemical Society*, 135 (2013) 3764-3767.

361 [16] T.J. Woehl, K.L. Jungjohann, J.E. Evans, I. Arslan, W.D. Ristenpart, N.D. Browning,
 362 Experimental procedures to mitigate electron beam induced artifacts during in situ fluid
 363 imaging of nanomaterials, *Ultramicroscopy*, 127 (2013) 53-63.

364 [17] H. Zheng, S.A. Claridge, A.M. Minor, A.P. Alivisatos, U. Dahmen, Nanocrystal
 365 diffusion in a liquid thin film observed by in situ transmission electron microscopy, Nano
 366 letters, 9 (2009) 2460-2465.

367 [18] M. Williamson, R. Tromp, P. Vereecken, R. Hull, F. Ross, Dynamic microscopy of
 368 nanoscale cluster growth at the solid–liquid interface, Nature materials, 2 (2003) 532.

369 [19] H. Zheng, R.K. Smith, Y.-w. Jun, C. Kisielowski, U. Dahmen, A.P. Alivisatos,
 370 Observation of single colloidal platinum nanocrystal growth trajectories, Science, 324 (2009)
 371 1309-1312.

372 [20] N. De Jonge, F.M. Ross, Electron microscopy of specimens in liquid, Nature
 373 nanotechnology, 6 (2011) 695.

374 [21] B.H. Kim, J. Yang, D. Lee, B.K. Choi, T. Hyeon, J. Park, Liquid-phase transmission
 375 electron microscopy for studying colloidal inorganic nanoparticles, Advanced Materials, 30
 376 (2018) 1703316.

377 [22] I. Fernando, Y. Zhou, Concentration dependent effect of humic acid on the
 378 transformations of silver nanoparticles, Journal of Molecular Liquids, 284 (2019) 291-299.

379 [23] J. Lu, Z. Aabdin, N.D. Loh, D. Bhattacharya, U. Mirsaidov, Nanoparticle dynamics in a
 380 nanodroplet, Nano letters, 14 (2014) 2111-2115.

381 [24] E. White, M. Mecklenburg, B. Shevitski, S. Singer, B. Regan, Charged nanoparticle
 382 dynamics in water induced by scanning transmission electron microscopy, Langmuir, 28
 383 (2012) 3695-3698.

384 [25] E.A. Ring, N. de Jonge, Video-frequency scanning transmission electron microscopy of
 385 moving gold nanoparticles in liquid, Micron, 43 (2012) 1078-1084.

386 [26] J. Liu, Z. Wang, A. Sheng, F. Liu, F. Qin, Z.L. Wang, In Situ Observation of Hematite
 387 Nanoparticle Aggregates Using Liquid Cell Transmission Electron Microscopy,
 388 Environmental Science & Technology, 50 (2016) 5606-5613.

- [27] N. Schneider, F. Ross, Electron beam effects in liquid cell TEM and STEM, *Liquid Cell Electron Microscopy*, (2016) 140.
- [28] P. Ngabonziza, M. Stehno, G. Koster, A. Brinkman, *In-Situ Characterization Techniques for Nanomaterials*, 1 ed., Springer 2018.
- [29] T. Woehl, P. Abellan, Defining the radiation chemistry during liquid cell electron microscopy to enable visualization of nanomaterial growth and degradation dynamics, *Journal of microscopy*, 265 (2017) 135-147.
- [30] W.R. Bowen, A.O. Sharif, Long-range electrostatic attraction between like-charge spheres in a charged pore, *Nature*, 393 (1998) 663.
- [31] B.M. Angel, G.E. Batley, C.V. Jarolimek, N.J. Rogers, The impact of size on the fate and toxicity of nanoparticulate silver in aquatic systems, *Chemosphere*, 93 (2013) 359-365.